Anal. Chem. **2007,** *79,* 6760−6766

Ruthenium Purple-Mediated Microelectrode Biosensors Based on Sol−Gel Film

Faming Tian, Enrique Llaudet, and Nicholas Dale*

Warwick Biosensors Group, Department of Biological Sciences, University of Warwick, Coventry, CV4 7AL, United Kingdom

Ruthenium Purple (RP), an analogue of Prussian Blue, has potentially advantageous electrochemical characteristics. We now demonstrate its use in microelectrode biosensors for the first time. An RP layer was grown on, and remained stably anchored to, the surface of gold microelectrodes at physiological pH ranges. Crucially, it retained its electrochemical activity in sodium-based phosphate buffers. The RP microelectrodes displayed electrocatalytic reduction of hydrogen peroxide at 0 to −50 mV (vs Ag/AgCl). To fabricate biosensors on the RP microelectrodes, we used a sol−gel film electrodeposition technique to create ATP and hypoxanthine biosensors as examples of the methodology. These RP-mediated biosensors displayed excellent performance including the following: high selectivity against interferences such as 5HT, ascorbic acid, urate, and acetaminophen; high sensitivity with wide linear calibration range; and good stability. These attractive characteristics demonstrate that RP can be universally employed as an electron mediator in fabrication of highly selective oxidase-based microelectrode biosensors. Furthermore, given their ability to operate in the presence of physiological levels of Na^+, the RP-mediated biosensors can be potentially applied to the in vitro and in vivo measurement of physiological signaling substances.

Amperometric biosensors based on enzymes continue to be a topic of interest due to their high selectivity and sensitivity. Miniaturized biosensors have been used for real-time measurements of analytes such as glucose, adenosine, ATP, and lactate in a range of clinical and physiological studies.[1−7] For those biosensors based on oxidases, the amperometric signal can most readily be obtained by monitoring the formation of hydrogen peroxide, a reaction product generated in the enzymatic layer. Traditionally, a relatively high anodic potential (>0.6 V, Ag/AgCl)[8] is required to oxidize hydrogen peroxide to obtain a biosensor of sufficient sensitivity. However, many substances usually present in biological samples (such as ascorbate, urate) can also be electrochemically oxidized at such a potential causing a high level of nonspecific interference. Thus, the selectivity of the biosensor can be poor in such a detection mode.

To improve the selectivity of oxidase-based biosensors in substrate detection, electron mediators have been widely employed as the electrochemical transducer to circumvent the problem of high working potential. For instance, Prussian Blue,[9−13] known as an "artificial enzyme peroxidase", and its analogues (such as palladium hexacyanoferrate,[14] chromium hexacyanoferrate,[15] and cupric hexacyanoferrate[16]) exhibit a strong and preferential electrocatalytic action toward the enzymatically produced hydrogen peroxide at low potentials, while also displaying a lower response to coexisting oxidizable substances. However, the electrochemistry of Prussian Blue is highly affected by cations presented in buffer solution. Those cations (such as K^+, NH_4^+, Rb^+, and Cs^+) whose hydrated ions fit the Prussian Blue lattice (1.019 nm) can promote its electrochemistry. On the other hand, cations that do not fit this lattice such as Na^+, H^+, Ca^{2+}, and Mg^{2+} are considered as blocking ones.[17−19] As a result, biosensors that adopt Prussian Blue as an electron mediator necessarily use potassium-based phosphate buffer solutions as the supporting electrolyte. Prussian Blue-based biosensors can thus be restricted in their utilization for practical use, as sodium-based buffers or salines are essential as the supporting solution in clinical or physiological measurements. Furthermore, some enzymes also require the presence of divalent cations such as Mg^{2+} or Ca^{2+} for catalytic activity, and these ions would block

* Corresponding author. E-mail: n.e.dale@warwick.ac.uk. Tel: +44-24-7652-3729. Fax: +44-24-7657-2594.

(1) Llaudet, E.; Hatz, S.; Droniou, M.; Dale, N. *Anal. Chem.* **2005**, *77*, 3267−3273.
(2) Gourine, A. V.; Llaudet, E.; Dale, N.; Spyer, K. M. *Nature* **2005**, *436*, 108−111.
(3) Dale, N.; Hatz, S.; Tian, F.; Llaudet, E. *Trends Biotechnol.* **2005**, *23*, 420−428.
(4) Wang, B.; Li, B.; Deng, Q.; Dong, S. *Anal. Chen.* **1998**, *70*, 3170−3174.
(5) Compagnone, D.; Guilbault, G. G. *Anal. Chim. Acta* **1997**, *340*, 109−113.
(6) Dale, N.; Gourine, A. V.; Llaudet, E.; Bulmer, D.; Thomas, T.; Spyer, K. M. *J. Physiol.* **2002**, *544*, 149−160.
(7) Parra, A.; Casero, E.; Vaquez, L.; Pariente, F.; Lorenzo, E. *Anal. Chim. Acta* **2006**, *555*, 308−315.
(8) Guilbault, G. G.; Lubrano, G. J. *Anal. Chim. Acta* **1973**, *64*, 439−455.
(9) Karyakin, A. A.; Gitelmacher, O. V.; Karyakina, E. E. *Anal. Chem.* **1995**, *67*, 2419−2423.
(10) Karyakin, A. A.; Puganova, E. A.; Budashov, I. A.; Kurochkin, I. N.; Karyakina, E. E.; Levchenko, V. A.; Matveyenko, V. N.; Varfolomeyev, S. D. *Anal. Chem.* **2004**, *76*, 474−478.
(11) Karyakin, A. A.; Karyakina, E. E.; Gorton, L. *Anal. Chem.* **2000**, *72*, 1720−1723.
(12) Ricci, F.; Palleschi, G. *Biosens. Bioelectron.* **2005**, *21*, 389−407.
(13) Ricci, F.; Amine, A.; Palleschi, G.; Moscone, D. *Biosens. Bioelectron.* **2003**, *18*, 165−174.
(14) Iveković, D.; Milardović, S.; Grabarić, B. S. *Biosens. Bioelectron.* **2004**, *20*, 872−878.
(15) Lin, M. S.; Shih, W. C. *Anal. Chim. Acta* **1999**, *381*, 183−189.
(16) Wang, J.; Zhang, X.; Prakash, M. *Anal. Chim. Acta* **1999**, *395*, 11−16.
(17) Itaya, K.; Shoji, N.; Uchida, I. *J. Am. Chem. Soc.* **1984**, *106*, 3423−3429.
(18) Itaya, K.; Uchida, I.; Neff, V. D. *Acc. Chem. Res.* **1986**, *19*, 162−168.
(19) Rajan, K. P.; Neff, V. D. *J. Phys. Chem.* **1982**, *86*, 4361−4368.

10.1021/ac070822f CCC: $37.00
Published on Web 08/03/2007

the operation of Prussian Blue-based sensors. A recent exception to this is screen-printed planar glucose biosensor adopting Prussian Blue as an electron mediator.[20]

As an analogue of Prussian Blue, Ruthenium Purple (RP),[21] which is a ferric ruthenocyanide, shows flexible electrochemistry in all kinds of supporting electrolytes containing different cations. Though RP has similar structure with a lattice constant of 1.042 nm,[19] its electrochemical properties are slightly different from those of Prussian Blue. The electrochemistry of RP survives in sodium-based phosphate buffers and two pairs of interesting redox peaks can be observed.[22] A recent study has shown that RP can be synthesized in aqueous Na^+ electrolytic solution via electrochemical deposition,[23] raising the possibility that RP could be used as an electrochemical mediator in in vitro or in vivo biosensors. So far, RP has only been reported as electrocatalytic mediator in glucose biosensors based on RP containing zeolite-modified conductive SnO_2 glass[24,25] and on RP/industrial waste cinder hybrid-modified carbon paste electrodes.[26]

The sol−gel techniques are of particular interest for enzyme immobilization on surface- or bulk-modified electrodes since there are many attractive properties of sol−gel materials including low-temperature encapsulation, tunable porosity, negligible swelling, chemical inertness, physical rigidity, and favorable biocompatibility.[27,28] Sol−gel film-coated biosensors have attracted tremendous attention because of their fast response and ease of preparation. In this type of biosensor, the desired sol−gel film was traditionally prepared by dip-coating or spin-coating hydrolyzed sol on the surface of a suitable substrate. Sol−gel films can be prepared via electrochemical deposition.[1,29−32] At a sufficient cathodic potential, OH ions can be generated at the surface of an electrode and act as a catalyst to enhance the condensation and polymerization of hydrolyzed sol solution, providing a new methodology for forming sol−gel films on conductive substrates. Our group has developed this methodology to make it compatible with proteins such as enzymes and hence suitable for biosensor formation. We have successfully used these methods to construct a range of amperometric microelectrode biosensors.[1,2,32]

We now report the development of microelectrode biosensors based on a RP-coated gold electrode. In this paper, we directly electrodeposit RP onto the surface of a gold electrode from its aqueous solution. Then, a desired gel layer is formed on the RP-modified electrode using our controllable sol−gel deposition technique to fabricate amperometric biosensors. To demonstrate that RP can be universally used as electron mediator in construction of microelectrode biosensors and to describe the characteristics of such biosensors, we have made two different types of biosensors for ATP and hypoxanthine, respectively.

EXPERIMENTAL SECTION

Materials and Instrumentation. All silanes and other chemicals were obtained from Sigma-Aldrich. They were of analytical grade and used directly without any further purification. Glycerokinase (EC 2.7.1.30, GK) from *Escherichia coli* (∼50 units/mg of solid) was obtained from Fluka. Glycerol-3-phophate oxidase (EC 1.1.3.21, G3PO) from *Streptococcus thermophilus* (∼10 units/mg of solid) and xanthine oxidase (EC 1.1.3.22, XO) from microorganisms (8.6 units/mg of solid) were obtained from Sigma. Sodium phosphate buffer solution (4 mM, pH 7.4, containing 0.1M NaCl, 1 mM $MgCl_2$, and 2.5 mM glycerol) was prepared and used as the common supporting electrolyte unless specified otherwise. Fresh stock solutions of potential interferences (such as 5HT, ascorbic acid, dopamine, 4-acetaminophen, and urate) were prepared just before use in biosensor selectivity tests.

A CHI 660 workstation was used in electrodeposition, voltammetric, and amperometric experiments. A three-electrode cell equipped with a platinum foil counter electrode and a Ag/AgCl (saturated KCl) reference electrode was used. Gold microelectrodes (obtained from Sycopel International Ltd. with a diameter of 50 μm, a length of 2 mm, and a surface area of 1.36×10^{-3} cm^2) were employed as the working electrode in all experiments. The supporting solutions were degassed thoroughly for at least 15 min with pure N_2 except for those used in amperometric measurements. All experiments were carried out at room temperature.

Electrodeposition of RP. Cyclic scanning was employed in electrochemical deposition of RP. Prior to use, the working gold electrode was pretreated electrochemically in 1 M sulfuric acid by cycling between 0 and 1.5 V at a sweep rate of 50 mV/s until stable voltammograms for gold oxide formation and reduction were obtained. The treated gold electrode was repetitively cycled in a mixture of $FeCl_3$ (0.5 mM), $K_4Ru(CN)_6$ (0.5 mM), and KCl (0.1 M, pH 2) at a scan rate of 50 mV/s between 0.1 and 1.0 V. Then the purple-colored electrode was dipped into $RuCl_3$ solution (1 mM, containing 1 mM KCl, pH 2) for another two to four cycles under the same conditions.[33,34] The resulting RP-modified gold electrode was thoroughly rinsed with pure water and ready for further use.

Sol−Gel Film Coatings. Sol−gel films can be coated on the surface of the RP-modified electrode by electrodeposition utilizing either galvanostatic or potentiostatic methods that have been described in detail elsewhere.[1,32] In brief, silane precursors such as tetramethoxysilane and (3-aminopropyl)trimethoxysilane were prehydrolyzed with diluted hydrochloric acid. Then they were mixed with 50 mM Tris buffer to neutralize their pH. Additives such as KCl and $Ca(NO_3)_2$ were added into the mixture to produce a sufficient amount of OH^- around the working electrode used for the formation of gel film. Finally, the RP-modified gold electrode was cathodically polarized under galvanostatic conditions by using a current density of 1.27 mA/cm^2 or under potentiostatic conditions to between −900 and −1200 mV for 10-40 s in a small

(20) Ricci, F.; Moscone, D.; Tuta, C. S.; Palleschi, G.; Amine, A.; Poscia, A.; Valgimigli, F.; Messeri, D. *Biosens. Bioelectron.* **2005**, *20*, 1993−2000.
(21) Itaya, K.; Ataka, T.; Toshima, S. *J. Am. Chem. Soc.* **1982**, *104*, 3751−3752.
(22) Abe, T.; Toda, G.; Tajiri, A.; Kaneko, M. *J. Eletroanal. Chem.* **2001**, *510*, 35−42.
(23) Chen, S. M.; Hsueh, S. H. *J. Electrochem. Soc.* **2003**, *150*, D175−D183.
(24) Shyu, S. C.; Wang, C. M. *J. Electrochem. Soc.* **1998**, *145*, 154−158.
(25) Chen, C. F.; Wang, C. M. *J. Electroanal. Chem.* **1999**, *466*, 82−89.
(26) Zen, J. M.; Kumar, A. S.; Chung, C. R. *Anal. Chem.* **2003**, *75*, 2703−2709.
(27) Gill, I.; Ballesteros, A. *J. Am. Chem. Soc.* **1998**, *120*, 8587−8598.
(28) Wang, J. *Anal. Chim. Acta* **1999**, *399*, 21−27.
(29) Shacham, R.; Avnir, D.; Mandler, D. *Adv. Mater.* **1999**, *11*, 384−388.
(30) Deepa, P. N.; Kanungo, M.; Claycomb, G.; Sherwood, P. M. A.; Collinson, M. M. *Anal. Chem.* **2003**, *75*, 5399−5405.
(31) Collinson, M. M.; Moore, N.; Deepa, P. N.; Kanungo, M. *Langmuir* **2003**, *19*, 7669−7672.
(32) WO2004048603.
(33) Cataldi, T. R. I.; Benedetto, G. E.; Campa, C. *J. Electroanal. Chem.* **1997**, *437*, 93−98.
(34) Cataldi, T. R. I.; Benedetto, G. E.; *J. Electroanal. Chem.* **1998**, *458*, 149−154.

capillary filling with the sol mixture. This resulted in the surface of the RP-coated gold electrode being totally covered by a transparent and uniform gel layer.

Biosensors fabricated in the experiments are based on the following enzymatic mechanism:

For the ATP biosensor,

$$\text{ATP} + \text{glycerol} \xrightarrow{\text{GK}} \text{glycerol-3-phosphate} + \text{ADP}$$

$$\text{glycerol-3-phosphate} + \text{O}_2 \xrightarrow{\text{G3PO}} \text{glycerone phosphate} + \text{H}_2\text{O}_2$$

For the hypoxanthine biosensor,

$$\text{hypoxanthine} + \text{O}_2 \xrightarrow{\text{XO}} \text{xanthine} + \text{H}_2\text{O}_2$$

$$\text{xanthine} + \text{O}_2 \xrightarrow{\text{XO}} \text{urate} + \text{H}_2\text{O}_2$$

The biosensors were prepared using the same method except that mixtures of sol with different enzymes (glycerol kinase and glycerol-3-phophate oxidase used for ATP biosensor, xanthine oxidase used for hypoxanthine biosensor) were used for film deposition. Glycerol was also employed in some instances to stabilize the bioactivity of enzymes. The resulting RP-modified, sol−gel-derived biosensors were kept in Tris buffer (pH 7.4) containing 0.1 M NaCl, 1 mM $MgCl_2$, and 2 mM glycerol at 4 °C when not in use. These wet storage conditions completely preserved biosensor activity for a few days. For longer term storage, the biosensors were rinsed with pure water and dried prior to storage at 4 °C. These dried sensors were used for stability testing.

RESULTS AND DISCUSSION

Electrodeposition of RP on a Gold Electrode. Traditionally, there are two different ways to prepare RP by electrochemical deposition methods. First, RP can be electrodeposited onto the surface of electrodes such as Pt, glassy carbon, and conductive SnO_2 by galvanostatic polarization in a mixture of Fe^{3+} and $Ru(CN)_6^{3-}$. However, RP cannot be efficiently produced in this manner as $Ru(CN)_6^{3-}$ is unstable and was usually obtained by oxidizing $Ru(CN)_6^{4-}$ with chemicals (such as Ce(IV) or PbO_2). Fortunately, RP can also be directly electroproduced in a mixture of Fe^{3+} and $Ru(CN)_6^{4-}$.[23,33] The soluble form of $Fe^{III}-Ru^{II}(CN)_6$ can be reduced to $Fe^{II}-Ru^{II}(CN)_6$ in such a method and thus subsequently deposited on the electrode surface.

By repetitively sweeping from 0.1 to 1.0 V at a scan rate of 50 mV/s, RP was electrodeposited onto the surface of gold electrode gradually (Figure 1A). It can be seen that the peak currents of both cathodic and anodic waves increased periodically with scan, which indicates that RP was electrodeposited onto the electrode surface step by step. During the first several scans, two pairs of redox peaks were observed. After ~30 cycles, only one pair of well-defined redox waves was left with a mean potential $E_{1/2} = (E_{pa} + E_{pc})/2$ of 297.3 mV and potential separation ΔE_p between the anodic and cathodic peaks of 60.6 mV. Further cyclic sweeps decreased the peak current, suggesting a saturated covering amount of RP on the gold electrode surface. The subsequent

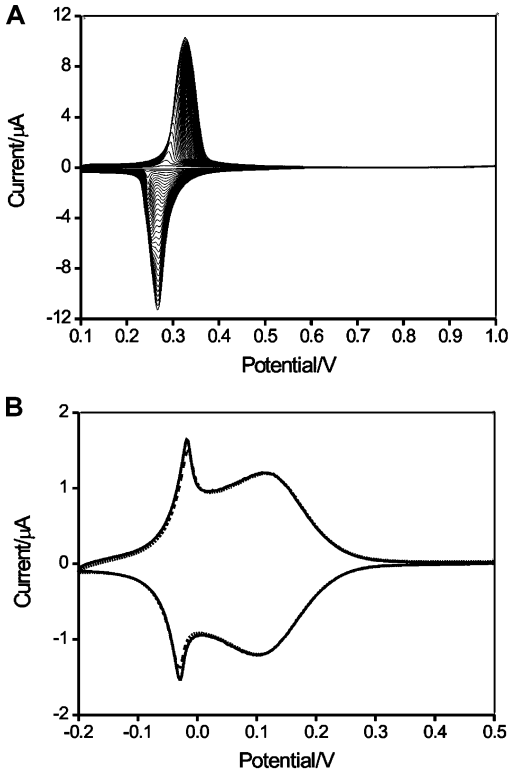

Figure 1. (A) Growth of RP on the surface of a gold electrode; (B) Comparison of the CVs of a RP-modified electrode scanned in phosphate buffer before (solid) and after (dash) gel deposition. Scan rate, 50 mV/s.

reduction of peak current may be caused by the semiconductive nature of the RP layer as it grew thicker. As a result, all RP-modified gold electrodes used in the study were totally covered with a saturating amount to give a shiny purple surface.

Electrochemistry of RP within Sol−Gel-Derived Gold Electrodes. A sol−gel film can be successfully deposited onto the surface of a RP-coated gold electrode using our controllable sol−gel deposition method. A purple inner layer and a transparent gel layer were clearly observed after the electrode was polarized at +500 mV, suggesting that sol−gel formation was unaffected by the underlying RP layer. Equally, RP was well retained on the surface of the gold electrode without any significant loss caused by the gel deposition process, as demonstrated by cyclic voltammograms (CVs) of the RP-modified gold electrodes scanned before and after the gel layer deposition (Figure 1B). To test whether the electrochemistry of RP was affected by the sol−gel film coating, we next examined its electrochemical behavior and electrocatalytic activity toward hydrogen peroxide.

Compared to potassium-based solutions, RP shows a different electrochemical behavior in supporting electrolytes containing sodium cations. As shown previously, RP shows only one pair of redox peaks with supporting electrolytes based on lattice-fitting cations (such as K^+ and NH_4^+). However, two pairs of redox peaks relating to RP electrochemistry were observed in sodium-based solutions, which is similar to the electrochemical performance exhibited by other Prussian Blue analogues.[35] Figure 2 displays

(35) Joseph, J.; Gomathi, H.; Rao, G. P. *J. Electroanal. Chem.* **1997**, *431*, 231−235.

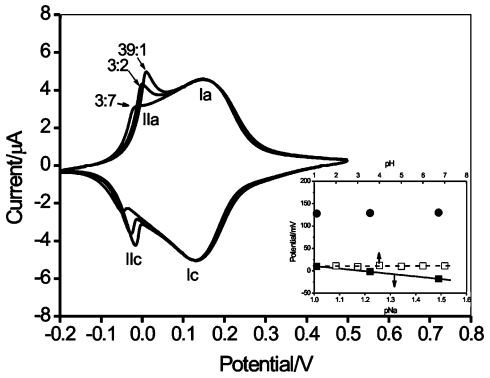

Figure 2. CVs of a gel-coated, RP-modified microelectrode in phosphate buffer with different ratios of Na^+/K^+ (total monovalent concentration of 100 mM), pH 2.0. Inset shows dependence of peak potential on pNa (E_{IIa} filled square, solid line) and pH (E_{IIa} open square, dashed line; E_{Ic} filled circle).

typical CVs at RP-modified sol−gel film (without enzyme)-coated gold electrode in an electrolyte solution containing NaCl and KCl with different ratios between them in a total concentration of 0.1 M. Despite the different concentrations of K^+ and Na^+ in these solutions, the mean peak potential of redox peak I occurred at 140.3 mV with a peak potential separation of 18.2 mV. For this pair of peaks, we suggest a four-electron involved process:[22]

$$Fe_4^{III}[Ru(CN)_6]_3 + 4e^- = Fe_4^{II}[Ru(CN)_6]_3^{4-}$$

However, the electrochemistry of redox peak II may be a cation-related process. Both cathodic and anodic peak currents increased with the increment of Na^+ concentration. At the same time, the redox peak potentials were shifted positively with a separation of ~27.3 mV. The oxidation potential of peak II showed a pNa ($pNa = -\log[Na^+]$) dependence of −58.4 mV/pNa, and it was also independent of the pH of the supporting electrolyte (Figure 2, inset). These results indicate that Na^+ takes part in the electrochemical process of redox peak II:[17,19,25]

$$K_2Fe_2^{III}Fe_2^{II}[Ru(CN)_6]_3 + 2Na^+ + 2e^- = Na_2K_2Fe_4^{II}[Ru(CN)_6]_3$$

Although the redox potential of peak II varied with the concentration of Na^+, the operational potential of RP-modified biosensors was not affected in physiological buffer solutions, which will be shown later.

Figure 3 depicts cyclic voltammograms of RP-modified, sol−gel-derived gold electrode in sodium-based phosphate buffer at different scan rates. At low scan rate (≤100 mV/s), a linear dependence of peak current (i_p) on scan rate (v) was obtained and shown in inset of Figure 3. It suggests a reversible, diffusionless, and surface electron-transfer process of RP on the electrode at low scan rate. The relationship between the peak current and scan rate is as follows:[36]

$$i_p = n^2F^2A\Gamma v/4RT$$

where Γ and A represent the surface coverage concentration of the electrode reaction substance and the electrode area, respectively. The symbols n, F, R, and T have their usual meanings. The RP surface coverage concentration was calculated as 3.34×10^{-10} mol/cm^2 from results shown in the inset. This is six times bigger than that reported on RP−clay-modified electrodes (5×10^{-11} mol/cm^2).[24]

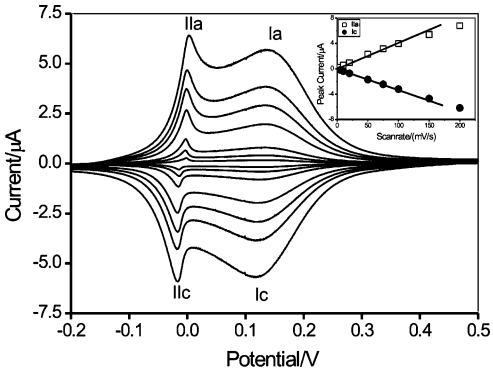

Figure 3. CV of a gel-coated RP-modified gold electrode in phosphate buffer (pH 7.4, NaCl 0.1 M) with different scan rates: 5, 10, 20, 50, 75, 100, and 150 mV/s. Inset shows dependence of peak currents on scan rates.

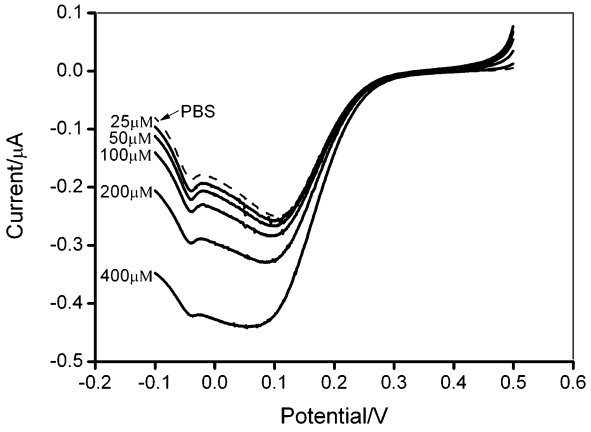

Figure 4. Linear sweep voltammograms of a gel-coated, RP-modified gold electrode in phosphate buffer (pH 7.4, NaCl 0.1 M) with and without hydrogen peroxide at concentrations of 25, 50, 100, 200, and 400 μM. Scan rate, 10 mV/s.

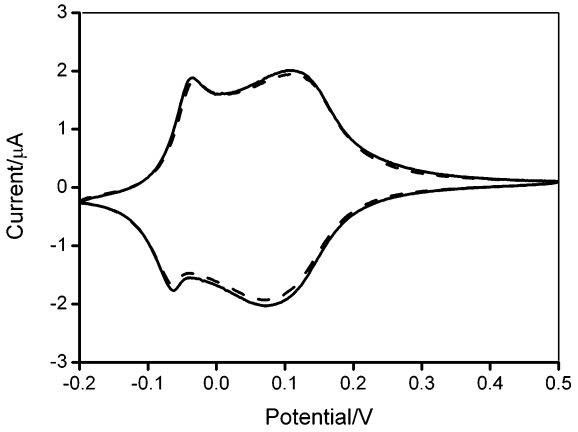

Figure 5. Comparison of the CVs of a RP-modified biosensor scanned before (solid) and after (dash) successive tests in a flowing system with 10 μM H_2O_2 for 1 h. Scan rate, 50 mV/s; other conditions are as in Figure 4.

(36) Brown, A. P.; Anson, F. C. *Anal. Chem.* **1977**, *49*, 1589−1595.

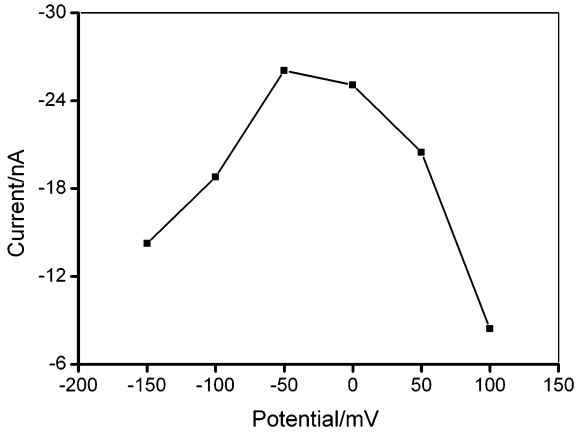

Figure 6. Dependence of response of an ATP biosensor on applied potential. ATP concentration, 50 μM.

Linear sweep voltammetry was employed to study the electrocatalytic action of RP on hydrogen peroxide. As with Prussian Blue and its other analogues, RP exhibited dramatic electrocatalysis toward hydrogen peroxide (Figure 4). With each increment of hydrogen peroxide concentration in phosphate buffer, the sensing response of RP-modified electrode increased correspondingly. The cathodic response to hydrogen peroxide occurred between potentials of +150 and −100 mV. This potentially allows highly selective operation of oxidase-based biosensors as small operational potentials can be selected to avoid amperometric responses to coexisting interferences.

In addition to the pH stability shown in the inset of Figure 2, RP exhibits stable immobilization on the surface of gold electrodes. RP-modified, sol−gel-derived gold microelectrodes were successively tested using 10 μM hydrogen peroxide in a flowing system for 1 h and their CVs recorded and compared (Figure 5). This demonstrates that RP was safely anchored and retained on the surface of gold microelectrodes although a very small reduction in CV amplitude was observed in the process.

We have thus shown that sol−gel layers can be easily formed on the surface of a RP-modified gold electrode by cathodic electrodeposition. The RP was not lost during the deposition process, retained its electrochemical properties, and allowed efficient electrocatalytic reduction of hydrogen peroxide at favorable operational potentials.

RP-Based, Sol−Gel-Derived Amperometric Biosensors. To illustrate the utility of RP for microelectrode biosensor fabrication, we doped enzyme(s) into hydrolyzed sol mixture to make two different types of biosensor for ATP and hypoxanthine. The performance (such as sensitivity and selectivity) of mediated biosensors relies greatly on the operational potential of the electron mediator. The ATP biosensor was employed to determine the optimum operational potential of RP-mediated, sol−gel-derived amperometric biosensors. Figure 6 displays dependence on the operational potential of responses to 50 μM ATP. As the electrode operational potential becomes more negative, the biosensor gradually gains its power to reduce the mediator oxidized by hydrogen peroxide. The optimized operational potential occurred in a wide range from −75 to 25 mV, and the ATP biosensor showed its best performance at −50 mV.

Biosensor Performance. As our mild gel layer deposition methods are excellent for retention of high enzymatic activities,

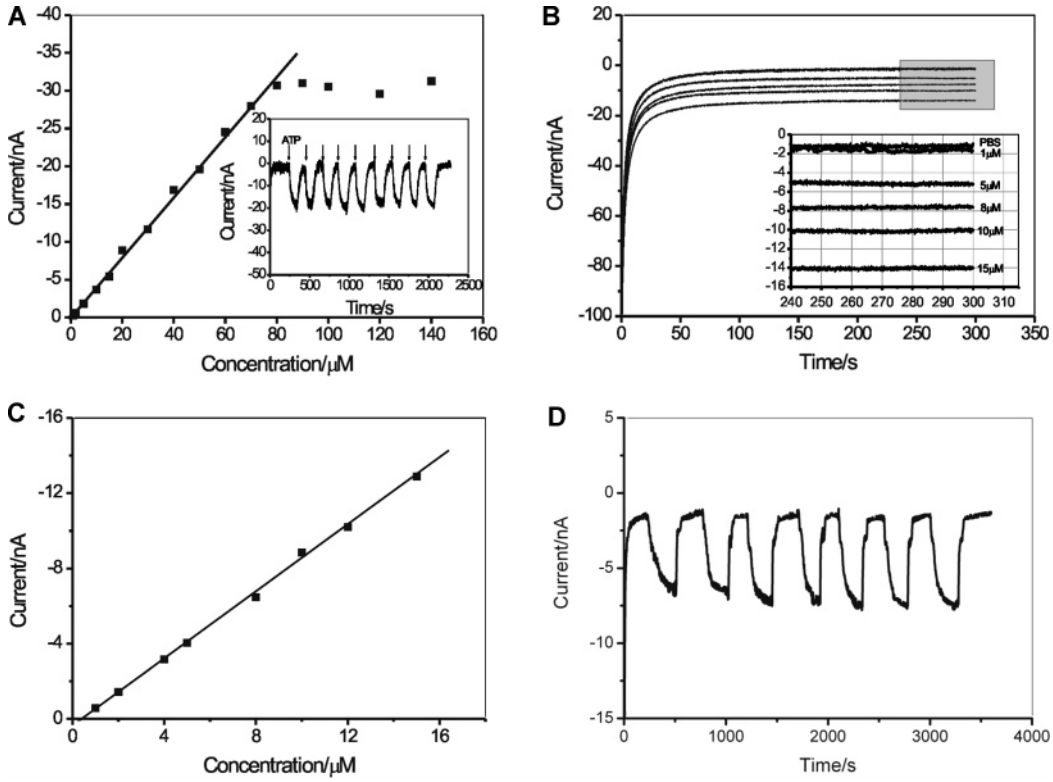

Figure 7. Amperometric performance of RP-modified biosensors in phosphate buffer (pH 7.4, NaCl 0.1 M). (A) Calibration of a typical ATP biosensor. Inset shows response of a typical biosensor to ATP (40 μM) in a flowing system. Operational potential, 0 mV. (B) Response of a hypoxanthine biosensor polarized at −50 mV in phosphate buffer with different concentrations of hypoxanthine (inset shows the enlargement of the highlighted region) and its corresponding calibration curve (C). (D) FIA response of an RP-modified hypoxanthine biosensor to hypoxanthine (10 μM). Applied potential, −50 mV.

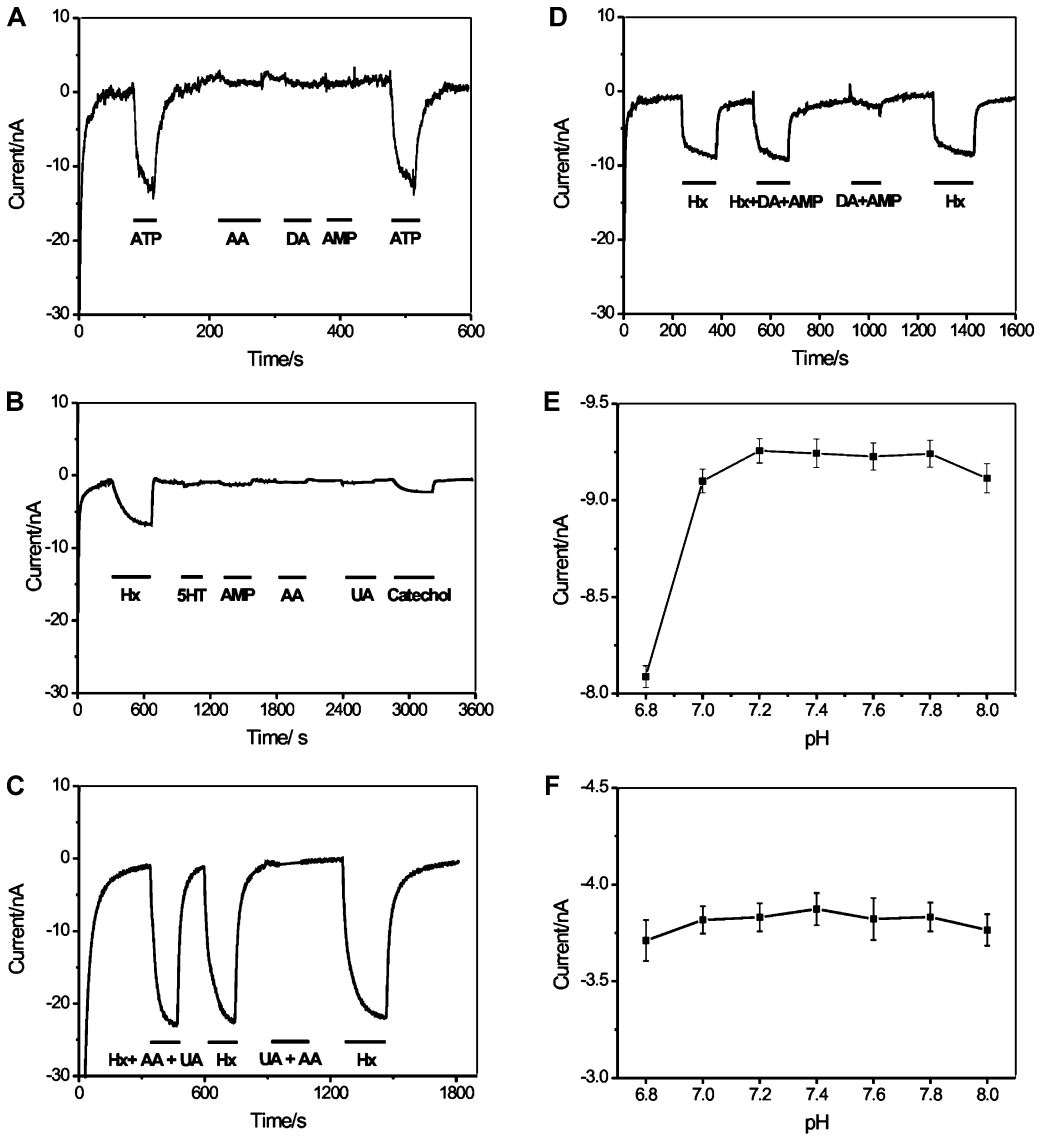

Figure 8. Selectivity and pH sensitivity. All experiments were performed in phosphate buffer (pH 7.4, NaCl 0.1 M) at −50 mV if without specification. (A) Response of an ATP biosensor to ATP (40 μM) and different interferences: ascorbic acid (AA, 40 μM), dopamine (DA, 40 μM), and 4-acetaminophen (AMP, 40 μM). (B) Response of a hypoxanthine (Hx) biosensor to Hx (10 μM) and different interferences: 5HT (100 μM), AMP (1 mM), AA (100 μM), uric acid (UA, 1 mM), and catechol (1 mM). (C) Dependence of hypoxanthine biosensor response on Hx (25 μM) and its mixture with UA (1 mM) and AA (100 μM). Applied potential, 0 mV. (D) Dependence of hypoxanthine biosensor response on Hx (10 μM) and its mixture with DA (100 μM) and AMP (100 μM). Applied potential, 0 mV. (E) Effect of buffer pH on response of hypoxanthine biosensor to 10 μM hypoxanthine, $n = 8$. (F) Effect of buffer pH on response of ATP biosensor to 10 μM ATP, $n = 5$.

the RP-mediated, sol−gel-derived biosensors show highly sensitive performance in detecting the corresponding substrate. In a flow system, the amperometric response of the ATP biosensor was recorded for injection of 40 μM ATP. The resulting $i-t$ curve and the calibration plot of the corresponding biosensor are shown in Figure 7A. The 10−90% response rise time was estimated as 33 ± 2 s ($n = 8$) for RP-mediated ATP biosensors. Although somewhat lower than ATP biosensors fabricated on nonmediated Pt microelectrodes,[1] the RP-mediated ATP biosensors still showed high sensitivity to ATP of 126 nA μM^{-1} cm^{-2} and a linear range from 0.3−80 μM.

For the hypoxanthine biosensor, responses were measured by polarizing the biosensor in phosphate buffer without and with different concentrations of hypoxanthine at −50 mV (Figure 7B). The cathodic response of the biosensor increased with the increment of hypoxanthine concentration in phosphate buffer with a relatively fast sensing speed (<20 s). The dependence of the response on hypoxanthine concentration gives a straight line from 0.2 μM up to 40 μM with a sensitivity of 334 nA μM^{-1} cm^{-2} (Figure 7C). The amperometric $i-t$ curve of the hypoxanthine biosensor recorded in a flowing system was highly stable (Figure 7D). During 1 h of successive testing, the biosensor showed a stable response to hypoxanthine, which is similar to that exhibited by the ATP biosensor (inset of Figure 7A). These results confirm that the enzymatic activity in the outer gel film is not affected by the inner RP layer in the configuration of biosensors and that RP is safely entrapped on the surface of gold electrode to electrocatalyze hydrogen peroxide produced during the biorecognition process.

Selectivity and Stability. The low operational potential makes it possible that RP-mediated biosensors are free of interference caused by coexisting substances in physiological samples. As

might be expected, equivalent concentrations (40 μM) of ascorbic acid, dopamine, and 4-acetaminophen showed no interfering signals on RP-mediated ATP biosensors, which gave dramatic responses to 40 μM ATP at −50 mV (Figure 8A). Further potential interfering substances were tested on a RP-mediated hypoxanthine biosensors (Figure 8B). With hypoxanthine biosensors, responses to 5HT (100 μM), ascorbic acid (100 μM), acetaminophen (1 mM), and uric acid (1 mM) were dramatically eliminated. A response of 1.58 nA for 1 mM catechol was observed. However, catechol is highly reactive and is unlikely to be present in physiological media. Even when an operational potential of 0 mV is used, the RP-modified hypoxanthine biosensors effectively rejected interferences. As shown in Figure 8C and D, the response of hypoxanthine on RP-mediated biosensor was not affected by either a mixture of 100 μM ascorbic acid and 1 mM uric acid or one of 100 μM dopamine and 100 μM 4-acetaminophen. The result of Figure 8C and D also indicates that selective detection can be achieved in a wide potential range. Thus, RP-modified, sol−gel-derived biosensors exhibit excellent selectivity while retaining excellent sensitivity to their analytes.

For amperometric biosensors, there are two key elements that could be affected by the pH of supporting buffer: the electron mediator and the enzyme(s). We have previously shown that the electrocatalysis of RP toward hydrogen peroxide is not affected by the pH of the electrolyte (inset of Figure 2). However, pH could affect the bioactivity of enzyme(s) immobilized in the sol−gel membrane. We therefore tested the sensitivity of responses of RP-mediated biosensors to their corresponding substrate to buffer pH. Figure 8E depicts such an effect of pH on response of a RP-mediated hypoxanthine biosensor to 10 μM hypoxanthine. And dependence of ATP biosensor response on 10 μM ATP is shown in Figure 8F. Both results suggest that the RP-mediated, sol−gel-derived biosensor displays a stable response over a wide physiological pH range from 7.0 to 8.0.

Besides the pH stability, the RP-mediated, sol−gel-derived biosensors also exhibit favorable stability in long-term storage. For instance, more than 95% sensitivity was retained for RP-mediated, sol−gel-derived ATP biosensors during 3 months of dry storage. Sol−gel bioencapsulation, especially under our mild chemical deposition conditions, retains the activity of enzyme(s) entrapped within the sol−gel layer of biosensor. Further attributes such as the rigidity, porosity, and hydrophilicity of sol−gel matrixes may also contribute to long-term stability. Furthermore, as demonstrated, the inner RP layer did not interfere with the bioactivity of enzyme(s) immobilized within the outer gel layer of the RP-mediated, sol−gel-derived biosensors.

CONCLUSIONS

Ruthenium Purple was successfully electrodeposited onto the surface of gold microelectrodes from aqueous solution. The immobilized RP displayed its tolerant electrochemistry and electrocatalytic behavior to hydrogen peroxide in a sodium-based phosphate buffer. Sol−gel-derived biosensors were further fabricated based on RP-modified gold microelectrodes using our mild chemical deposition method. Surprisingly, formation of the gel film was not affected by the inner RP layer. As a result, bioactivity of enzymes entrapped in gel film was well retained, even in long-term storage. The resulting biosensors had highly attractive performance characteristics including high sensitivity, wide linear calibration range, and excellent selectivity versus interferences. We have shown that, in principle, RP can be universally employed as electron mediator in fabrication of oxidase-based microelectrode biosensors, which could be widely applied to the in vitro and in vivo measurement of physiological substances.

ACKNOWLEDGMENT

We thank the Wellcome Trust for generous support.

SUPPORTING INFORMATION AVAILABLE

Video of Ruthenium Purple-modified sol−gel film-coated microbiosensor recorded with CV scanned from −0.2 to 0.4 V (vs AgCl/Ag) for two cycles. This material is available free of charge via the Internet at http://pubs.acs.org.

Received for review April 24, 2007. Accepted July 3, 2007.

AC070822F